

Regularization of covariance matrices on Riemannian manifolds using linear systems

Lipeng Ning

Abstract

We propose an approach to use the state covariance of linear systems to track time-varying covariance matrices of non-stationary time series. Following concepts from Riemannian geometry, we investigate three types of covariance paths obtained by using different quadratic regularizations of system matrices. The first quadratic form induces the geodesics based on the Bures-Wasserstein metric from optimal mass transport theory and quantum mechanics. The second type of quadratic form leads to the geodesics based on the Fisher-Rao metric from information geometry. In the process, we introduce a fluid-mechanics interpretation of the Fisher-Rao metric for multivariate Gaussian distributions. A main contribution of this work is the introduction of the third type of covariance paths which are steered by linear system matrices with rotating eigenspace. We provide theoretical results on the existence and uniqueness of this type of covariance paths. The three types of covariance paths are compared using two examples with synthetic data and real data based on functional magnetic resonance imaging, respectively.

Index Terms

System identification; Riemannian metric; optimal mass transport; information theory; optimal control; brain networks; functional MRI

I. INTRODUCTION

The problem of tracking changes and deformations of positive definite matrices is relevant to a wide spectrum of scientific applications, including computer vision, sensor array, and diffusion tensor imaging, see e.g. [1]–[7]. A key motivation behind the present work is from a neuroscience application on understanding functional brain connectivity using resting-state

L. Ning is with the Department of Psychiatry, Brigham and Women’s Hospital, Harvard Medical School. Email: lning@bwh.harvard.edu

function MRI (rsfMRI) data. Specifically, rsfMRI is a widely used neuroimaging modality which acquires a sequence three-dimensional image volumes from the whole brain to understand brain functions and activities [8]. The standard approach for analyzing the interdependence between brain regions is to compute the correlation coefficient between the underlying rsfMRI time-series data. Typically, the whole-brain functional network is characterized by the covariance matrix of a multivariate time-series data obtained from different brain regions [9], [10]. It has been recently observed that the functional connectivity fluctuates over time [11], [12], implying that the static covariance matrix based on the assumption of stationary time series may be too simplistic to capture the full extent of brain activities. Thus there is an urgent need for new computational tools for understanding dynamic functional brain networks using non-stationary rsfMRI data.

The aim of this work is use control-theoretic approaches to develop models for time-varying covariance matrices. In particular, we consider a non-stationary, discrete-time random process as observations of a zero-mean time-dependent random variable $\mathbf{x}_t \in \mathbb{R}^n$. We assume that the temporal change of the probability distributions $p_t(\mathbf{x})$ of \mathbf{x}_t is much slower than the rate of measurements. Therefore, the instantaneous covariance matrix

$$P_t := \mathcal{E}_{p_t}(\mathbf{x}\mathbf{x}') = \int_{\mathbb{R}^n} \mathbf{x}\mathbf{x}' p_t(\mathbf{x}) d\mathbf{x},$$

can be estimated by using sample covariance matrices computed from measurements from short time windows. Assume that two covariance matrices P_0 and P_1 at $t = 0, 1$ are known. Then geodesics connecting P_0 and P_1 on the manifold of positive-definite matrices provide natural structures to model time-varying covariance matrices P_t on the time interval $t \in [0, 1]$. As generalizations of straight lines in Euclidean space, geodesics are paths of shortest distances connecting the start to the finish on a curved manifold. The path length is measured by Riemannian metrics which are quadratic forms of the tangent matrix \dot{P}_t . Several Riemannian metrics have been proposed to derive geodesics for covariances matrices. For instance, the geodesics based on the Fisher-Rao metric for Gaussian distributions [13]–[16] from the theory of information geometry is given by

$$P_t^{\text{info}} = P_0^{1/2} (P_0^{-1/2} P_1 P_0^{-1/2})^t P_0^{1/2}. \quad (1)$$

An other example would be the Wasserstein-2 metric for Gaussian probability density functions

[17]–[20], which induces the following geodesic

$$P_t^{\text{omt}} = \left((1-t)P_0^{\frac{1}{2}} + tP_1^{\frac{1}{2}}\hat{U} \right) \left((1-t)P_0^{\frac{1}{2}} + tP_1^{\frac{1}{2}}\hat{U} \right)', \quad (2)$$

where $P_t^{\frac{1}{2}}$ denotes the unique positive-definite square root of P_t , and

$$\hat{U} = P_1^{-1/2} P_0^{-1/2} (P_0^{1/2} P_1 P_0^{1/2})^{1/2}$$

is an orthogonal matrix. These Riemmanian metrics will be explained in more details in the following sections.

In this paper, we combine concepts from Riemmanian geometry and linear systems to develop smooth covariance paths. Specifically, we consider a geodesic P_t as the state covariance of the following linear system

$$\dot{\mathbf{x}}_t = A_t \mathbf{x}_t, \quad (3)$$

with $A_t \in \mathbb{R}^{n \times n}$. We analyze the linear systems that steer P_t along different geodesics. Based on (3), the state covariance evolves according to

$$\dot{P}_t = A_t P_t + P_t A_t'. \quad (4)$$

Thus, the matrix A_t can be considered as a non-commutative deviation of \dot{P}_t by P_t scaled by a factor of $\frac{1}{2}$. Clearly, if P_t is given, the mapping from A_t to \dot{P}_t induced by (4) is injective. In this paper, we consider the A_t that the minimizer of a quadratic function $f(A_t)$ such that (4) holds. The optimal value $f(A_t)$ provides an alternative way to define Riemannian metrics for measuring the length of covariance paths. To this end, we consider covariance paths that are the solutions to

$$\min_{P_t, A_t} \left\{ \int_0^1 f(A_t) dt \mid \dot{P}_t = A_t P_t + P_t A_t', P_0, P_1 \text{ given} \right\}. \quad (5)$$

Note that the optimal system matrix A_t may not be symmetric, which could provide useful information to understand directed interactions among the underlying variables. In this work, we investigate the solution to (5) with three different types of quadratic forms of $f(A_t)$. The first two quadratic forms lead to the geodesic paths P_t^{omt} and P_t^{info} , respectively. A main contributions of this work in the introduction of the third family of geodesics which are the state covariances of linear system with rotating eigespace.

This paper is organized as follows. In Section II, we revisit the OMT-based geodesics P_t^{omt} and introduce the corresponding quadratic form $f(A_t)$. Section III will focus on the quadratic forms that lead to the Fisher-Rao-based geodesics P_t^{info} . We also introduce a fluid-mechanics interpretation of the Fisher-Rao metric, which provides a point of contact between OMT and information geometry. In Section IV, we investigate the optimal solutions to (5) corresponding to a family of quadratic functions $f(A_t)$ which are weighted-square norms of the symmetric and asymmetric part of A_t . We provide the expression of the optimal solutions and analysis on the existence and uniqueness of the solutions. In Section V, we compare the three types of covariances paths using two examples based on synthetic data and real data from rsfMRI, respectively. Section VI includes the discussions and conclusions.

For notations, $\mathbb{S}^n, \mathbb{S}_+^n, \mathbb{S}_{++}^n$ denote the set of symmetric, positive semidefinite, and positive definite matrices of size $n \times n$, respectively. Small boldface letters, e.g. \mathbf{x}, \mathbf{v} , represent column vectors. Capital letters, e.g. P, A , denote matrices. Regular small letters, e.g. w, h are for scalars or scalar-valued functions.

II. MASS-TRANSPORT BASED COVARIANCE PATHS

A. On optimal mass transport

Let $p_0(\mathbf{x})$ and $p_1(\mathbf{x})$ denote two probability density functions on \mathbb{R}^n . The Wasserstein-2 metric between the two, denoted by $w_2(p_0, p_1)$, is defined by

$$\begin{aligned} w_2(p_0, p_1)^2 &= \inf_{m(\mathbf{x}, \mathbf{y}) \geq 0} \int_{\mathbb{R}^n \times \mathbb{R}^n} \|\mathbf{x} - \mathbf{y}\|_2^2 m(\mathbf{x}, \mathbf{y}) d\mathbf{x} d\mathbf{y}, \\ \text{s.t. } \int_{\mathbb{R}^n} m(\mathbf{x}, \mathbf{y}) d\mathbf{x} &= p_1(\mathbf{y}), \int_{\mathbb{R}^n} m(\mathbf{x}, \mathbf{y}) d\mathbf{y} = p_0(\mathbf{x}), \end{aligned}$$

where $m(\mathbf{x}, \mathbf{y})$ represents a probability density function on the joint space $\mathbb{R}^n \times \mathbb{R}^n$ with the marginals specified by p_0 and p_1 , [17], [18]. A fluid-mechanics interpretation of $w_2(p_0, p_1)^2$ was introduced in [25], [26], which provided a Riemmanian structure of the manifold of probability density functions. To introduce this formula, we consider the following continuity equation

$$\frac{\partial p_t(\mathbf{x})}{\partial t} + \nabla_{\mathbf{x}} \cdot (p_t(\mathbf{x}) \mathbf{v}_t(\mathbf{x})) = 0, \quad (6)$$

where $\mathbf{v}_t(\mathbf{x})$ represents a time-varying velocity field. Then, $w_2(p_0, p_1)^2$ is equal to [26]

$$w_2(p_0, p_1)^2 = \inf_{p_t, \mathbf{v}_t} \left\{ \int_0^1 \mathcal{E}_{p_t}(\|\mathbf{v}_t(\mathbf{x})\|_2^2) dt \mid \dot{p}_t + \nabla_{\mathbf{x}} \cdot (p_t \mathbf{v}_t) = 0 \right\}. \quad (7)$$

The optimal solution of $p_t(\mathbf{x})$ is the geodesic on the manifold of probability density functions that connects the endpoints $p_0(\mathbf{x})$ and $p_1(\mathbf{x})$.

B. The Bures-Wasserstein metric

In the special case when $p_0(\mathbf{x})$ and $p_1(\mathbf{x})$ are zero-mean Gaussian probability density functions with

$$p_i(\mathbf{x}) = \det(2\pi P_i)^{-\frac{1}{2}} e^{-\frac{1}{2}\mathbf{x}'P_i^{-1}\mathbf{x}}, \text{ for } i = 0, 1,$$

the corresponding geodesic $p_t(\mathbf{x})$ at any fixed time t is also zero-mean Gaussian with the corresponding covariance matrix given by P_t^{omt} [19], [20]. The geodesic distance is equal to Wasserstein-2 metric $w_2(p_0, p_1)$, which also induces the following distance measure on the covariance matrices

$$w_2(p_0, p_1) = d_{w_2}(P_0, P_1) := \|P_0^{\frac{1}{2}} - P_1^{\frac{1}{2}}\hat{U}\|_F, \quad (8)$$

where $\|\cdot\|_F$ denotes the Frobenius norm of a matrix.

The covariance path P_t^{omt} is also equal to the geodesic induced by the Bures metric from quantum mechanics [23], [24] on the manifold of positive definite matrices. In particular, let $P \in \mathbb{S}_{++}^n$ and $\Delta \in S_{ym_n}$ which represents a tangent vector at P . The Bures metric takes the form

$$g_{P, \text{Bures}}(\Delta) = \text{tr}(\Delta M),$$

where $M \in \mathbb{S}^n$ and $\frac{1}{2}(PM + MP) = \Delta$, see e.g. [21], [22]. The trajectory P_t^{omt} in (2) is the shortest path connecting P_0 and P_1 . Thus, it satisfies that

$$P_t^{\text{omt}} = \underset{P_t}{\text{argmin}} \int_0^1 g_{P_t, \text{Bures}}(\dot{P}_t) dt, \quad (9)$$

with a given pair of endpoints $P_0, P_1 \in \mathbb{S}_{++}^n$, see e.g. [23]. The geodesic distance, also known as the Bures distance, is equal to $d_{w_2}(P_0, P_1)$.

The Bures metric was originally proposed in quantum mechanics to compare density matrices, which are positive definite matrices whose traces are equal to one. The density matrices are non-commutative analogues of probability vectors. In the commutative case when P is restricted to be a diagonal matrix whose diagonal entries consist of a probability vector, then the Bures metric $g_{P, \text{Bures}}(\Delta)$ is equal the Fisher information metric which will be discussed in Section III.

C. Bures-Wasserstein-based linear systems

Here, we present an alternative expression of (9) using the linear system in (3). For this purpose, we define that

$$f_{P_t}(A_t) := \text{tr}(A_t P_t A_t'), \quad (10)$$

which is equal to $\mathcal{E}_{p_t}(\|\dot{\mathbf{x}}_t\|^2)$ if $\dot{\mathbf{x}}_t$ is given by (3). The following proposition relates the geodesics P_t^{omt} to a linear system.

Proposition 1. *Given $P_0, P_1 \in \mathbb{S}_{++}^n$. Then P_t^{omt} given by (2) is the unique minimizer of*

$$\min_{P_t, A_t} \left\{ \int_0^1 f_{P_t}(A_t) dt \mid \dot{P}_t = A_t P_t + P_t A_t', P_0, P_1 \text{ specified} \right\}, \quad (11)$$

with $f_{P_t}(A_t)$ defined by (10) and the optimal A_t is equal to

$$A_t^{\text{omt}} = Q(tQ - I)^{-1}, \quad (12)$$

where $Q = I - P_0^{-\frac{1}{2}}(P_0^{\frac{1}{2}}P_1P_0^{\frac{1}{2}})^{\frac{1}{2}}P_0^{-\frac{1}{2}}$. The optimal value of the objective function in (11) is equal to $d_{w_2}(P_0, P_1)^2$.

Proof. The optimization problem (11) takes a special form of (7) with $p_0(\mathbf{x}), p_1(\mathbf{x})$ being two zero-mean Gaussian probability density functions and an additional constraint that the velocity field $\mathbf{v}_t(\mathbf{x}) = A_t \mathbf{x}$. Thus, $d_{w_2}(P_0, P_1)^2$ is a lower bound of (11). Therefore, we only need to show that A_t^{omt} satisfies the constraint and provides the optimal value.

$$\dot{P}_t^{\text{omt}} = A_t^{\text{omt}} P_t^{\text{omt}} + P_t^{\text{omt}} (A_t^{\text{omt}})'. \quad (13)$$

First, we rewrite (2) as $P_t^{\text{omt}} = (I - tQ)P_0(I - tQ)$. Taking the derivative of P_t^{omt} gives

$$\begin{aligned} \dot{P}_t^{\text{omt}} &= -QP_0(I - tQ) - (I - tQ)P_0Q \\ &= Q(tQ - I)^{-1}P_t + P_tQ(tQ - I)^{-1}. \end{aligned}$$

Since all the eigenvalues of Q are smaller than 1, the matrix $tQ - I$ is invertible for all $t \in [0, 1]$.

Therefore (13) holds. Moreover,

$$\begin{aligned} \text{tr}(A_t^{\text{omt}} P_t^{\text{omt}} A_t^{\text{omt}}) &= \text{tr}(Q P_0 Q) \\ &= \|P_1^{1/2} \hat{U} - P_0^{1/2}\|_F^2 = d_{w_2}(P_0, P_1)^2, \end{aligned}$$

which completes the proof. \square

We note that the matrix A_t^{omt} is symmetric. Moreover, the matrices $A_{t_1}^{\text{omt}}$ and $A_{t_2}^{\text{omt}}$ commute for any t_1, t_2 . Therefore the eigenspace of A_t is fixed on the interval $t \in [0, 1]$.

The results from Proposition (1) can be further extended to obtain the optimal solutions corresponding to the following objective function

$$f_{P_t}^W(A_t) = \mathcal{E}_{p_t}(\|\dot{\mathbf{x}}_t\|_W^2) = \text{tr}(W A_t P_t A_t'), \quad (14)$$

where $\dot{\mathbf{x}}_t = A_t \mathbf{x}$, $W \in \mathbb{S}_{++}^n$ and $\|\dot{\mathbf{x}}_t\|_W^2 := \mathbf{x}' W \mathbf{x}$. By applying change of variables, we define

$$P_{W,t} := W^{\frac{1}{2}} P_t W^{\frac{1}{2}}, \quad (15)$$

$$A_{W,t} := W^{\frac{1}{2}} A_t W^{-\frac{1}{2}}. \quad (16)$$

Thus, $f_{P_t}^W(A_t) = \text{tr}(A_{W,t} P_{W,t} A_{W,t}') = f_{P_{W,t}}(A_{W,t})$. Moreover, if (4) holds, then

$$\dot{P}_{W,t} = A_{W,t} P_{W,t} + P_{W,t} A_{W,t}'.$$

Therefore, if A_t^{omt} is the optimal system matrix that steers $P_{W,0}$ to $P_{W,1}$ with respect to $f_P(A)$ given by Proposition 1, then $W^{-\frac{1}{2}} A_t^{\text{omt}} W^{\frac{1}{2}}$ is the optimal solution with respect to $f_P^W(A)$. In the following section, we investigate a further extension of $f_P^W(\cdot)$ by using a time-dependent weighting matrix which provides a point of contact between OMT and information geometry.

III. INFORMATION-GEOMETRY BASED COVARIANCE PATHS

A. The Fisher-Rao metric

For two probability density functions $p(\mathbf{x})$ and $\hat{p}(\mathbf{x})$ on \mathbb{R}^n , the Kullback-Leibler (KL) divergence

$$d_{\text{KL}}(p||\hat{p}) := \int_{\mathbb{R}^n} p \log \left(\frac{p}{\hat{p}} \right) d\mathbf{x} \quad (17)$$

represents a well-established notion of distance between the two [27], [28]. If $\hat{p} = p + \delta$ with δ representing a small perturbation, then the quadratic term of the Taylor's expansion of $d_{\text{KL}}(p||p+\delta)$ in terms of δ is the Fisher information metric

$$g_{p,\text{Fisher}}(\delta) = \int \frac{\delta^2}{p} d\mathbf{x}.$$

For a probability distribution $p(\mathbf{x}, \boldsymbol{\theta})$ parameterized by a vector $\boldsymbol{\theta}$, the corresponding metric is referred to as the Fisher-Rao metric and given by

$$g_{\boldsymbol{\theta},\text{Rao}}(\delta\boldsymbol{\theta}) = \delta\boldsymbol{\theta}' \mathcal{E} \left[\left(\frac{\partial \log p}{\partial \boldsymbol{\theta}} \right) \left(\frac{\partial \log p}{\partial \boldsymbol{\theta}} \right)' \right] \delta\boldsymbol{\theta}.$$

If $p(\mathbf{x})$ is a zero-mean Gaussian probability density function parameterized by a covariance matrix P , then the metric becomes

$$g_{P,\text{Rao}}(\Delta) = \text{tr}(P^{-1} \Delta P^{-1} \Delta).$$

Given $P_0, P_1 \in \mathbb{S}_{++}^n$, the geodesic in (1) is equal to the solution

$$P_t^{\text{info}} = \underset{P_t}{\text{argmin}} \int_0^1 g_{P,\text{Rao}}(\dot{P}_t) dt, \quad (18)$$

which is the shortest path connecting P_0 and P_1 . The corresponding path length is equal to

$$d_{\text{info}}(P_0, P_1) = \left\| \log(P_0^{-\frac{1}{2}} P_1 P_0^{-\frac{1}{2}}) \right\|_{\text{F}}, \quad (19)$$

see e.g. [29, Theorem 6.1.6]

B. Fisher-Rao metric based linear systems

Following (5), we will define a positive quadratic form so that the optimal state covariance is equal to P_t^{info} . One choice for the quadratic form would be given by

$$\begin{aligned} f_P^{\text{info},1}(A) &:= g_{P,\text{Rao}}(AP + PA') \\ &= 2\text{tr}(AA + P^{-1}APA'), \end{aligned} \quad (20)$$

which satisfies that $f_P^{\text{info},1}(A) \geq 0, \forall A \in \mathbb{R}^{n \times n}$ and $P \in \mathbb{S}_{++}^n$.

Proposition 2. Given $P_0, P_1 \in \mathbb{S}_{++}^n$, P_t^{info} from (1) is the unique minimizer of

$$\min_{P_t, A_t} \left\{ \int_0^1 f_{P_t}^{\text{info},1}(A_t) dt \mid \dot{P}_t = A_t P_t + P_t A_t', P_0, P_1 \text{ specified} \right\}, \quad (21)$$

with $f_{P_t}^{\text{info}}(A_t)$ defined by (20) and the optimal A_t is equal to

$$A^{\text{info}} := \frac{1}{2} P_0^{\frac{1}{2}} \log(P_0^{-\frac{1}{2}} P_1 P_0^{-\frac{1}{2}}) P_0^{-\frac{1}{2}}. \quad (22)$$

Moreover, the optimal value of the objective function is equal to $d_{\text{info}}(P_0, P_1)^2$.

Proof. We rewrite (1) as

$$\begin{aligned} P_t^{\text{info}} &= P_0^{\frac{1}{2}} (P_0^{-\frac{1}{2}} P_1 P_0^{-\frac{1}{2}})^t P_0^{\frac{1}{2}} \\ &= P_0^{\frac{1}{2}} e^{\frac{1}{2} \log(P_0^{-\frac{1}{2}} P_1 P_0^{-\frac{1}{2}}) t} e^{\frac{1}{2} \log(P_0^{-\frac{1}{2}} P_1 P_0^{-\frac{1}{2}}) t} P_0^{\frac{1}{2}} \\ &= e^{A^{\text{info}} t} P_0 e^{A^{\text{info}} t}, \end{aligned}$$

where the last equation is obtained using $e^{XYX^{-1}} = X e^Y X^{-1}$. Taking the derivative of P_t^{info} to give that

$$\dot{P}_t^{\text{info}} = A^{\text{info}} P_t^{\text{info}} + P_t^{\text{info}} A^{\text{info}'}, \quad (23)$$

which completes the proof. \square

Note that the metric $d_{\text{info}}(\cdot)$ is invariant with respect to congruence transforms, i.e. $d_{\text{info}}(P_0, P_1) = d_{\text{info}}(TP_0T', TP_1T')$ for any invertible matrix T . If A_t^{info} is the optimal solution of (21). Then $TA^{\text{info}}T^{-1}$ is the optimal solution corresponding to the pair TP_0T', TP_1T' .

C. A weighted-mass-transport view

Since the map from A_t to \dot{P}_t in (4) is injective, the quadratic forms of A_t that lead to P_t^{info} is not unique. Here, we provide an alternative form, which provides an interesting relation between OMT and the Fisher-Rao metric. For this purpose, we define the following weighted square norm

$$f_{P_t}^{\text{info},2}(A_t) = 4\mathcal{E}_{P_t}(\|\dot{\mathbf{x}}_t\|_{P_t^{-1}}^2) = 4\text{tr}(P_t^{-1} A_t P_t A_t'), \quad (24)$$

which is a special form of (14) with the weighting matrix $W = P_t$ and scaled by the factor of 4. The following lemma draws the relation between $f_P^{\text{info},2}(A)$ and $f_P^{\text{info},1}(A)$.

Lemma 1. Consider $f_P^{\text{info},1}(\cdot)$ and $f_P^{\text{info},2}(\cdot)$ be defined in (20) and (24), respectively. Then,

$$f_P^{\text{info},2}(A) \geq f_P^{\text{info},1}(A), \forall P \in \mathbb{S}_{++}^n, A \in \mathbb{R}^{n \times n}.$$

Proof. Taking the difference

$$\begin{aligned} & f_P^{\text{info},2}(A) - f_P^{\text{info},1}(A) \\ &= 2\text{tr}(P^{-1}APA' - AA) \\ &= \text{tr} \left((P^{-\frac{1}{2}}AP^{\frac{1}{2}} - P^{\frac{1}{2}}A'P^{-\frac{1}{2}})(P^{-\frac{1}{2}}AP^{\frac{1}{2}} - P^{\frac{1}{2}}A'P^{-\frac{1}{2}})' \right), \end{aligned}$$

which is non-negative. \square

We note that if $P^{-\frac{1}{2}}AP^{\frac{1}{2}}$ is symmetric, then $f_P^{\text{info},1}(A)$ is equal to $f_P^{\text{info},2}(A)$. This gives rise to the following proposition in parallel to Proposition 2.

Proposition 3. Given $P_0, P_1 \in \mathbb{S}_{++}^n$. Then $P_t^{\text{info}}, A^{\text{info}}$ given by (1) and (22), respectively, are the unique pair of minimizer of

$$\min_{P_t, A_t} \left\{ \int_0^1 f_{P_t}^{\text{info},2}(A_t) dt \mid \dot{P}_t = A_t P_t + P_t A_t', P_0, P_1 \text{ specified} \right\}, \quad (25)$$

with $f_{P_t}^{\text{info},2}(A_t)$ defined by (24).

Proof. From Lemma 1,

$$\int_0^1 f_{P_t}^{\text{info},2}(A_t) dt \geq \int_0^1 f_{P_t}^{\text{info},1}(A_t) dt \geq d_{\text{info}}(P_0, P_1)^2, \quad (26)$$

for any feasible pairs of P_t and A_t . It is straightforward to verify that the above inequalities become equalities with the given P_t^{info} and A^{info} . Therefore, the proposition holds. \square

D. A fluid-mechanics interpretation

Note that $f_{P_t}^{\text{info},2}(A_t)$ is a special case of $f_{P_t}^W(A)$ in (14) when $W = 4P_t^{-1}$. It is equal to

$$f_{P_t}^{\text{info},2}(A_t) = 4\mathcal{E}_{p_t}(\|\mathbf{v}_t(\mathbf{x})\|_{P_t^{-1}}^2),$$

with the velocity field given by $\mathbf{v}_t(\mathbf{x}) = A_t \mathbf{x}$. Thus if the initial distribution $p_0(\mathbf{x})$ is Gaussian, so is $p_t(\mathbf{x}), \forall t \geq 0$. Proposition (3) implies that among all the trajectories that connect two Gaussian probability density functions p_0 and p_1 , the lowest weighted-mass-transport cost is

obtained by Gaussian density functions whose covariance matrices are equal to P_t^{info} . But this optimal trajectory is obtained under the linear constraint of velocity fields. Next, we remove this constraint and show that this trajectory is still optimal.

Theorem 1. *Given two zero-mean Gaussian probability density functions $p_0(\mathbf{x}), p_1(\mathbf{x})$ on \mathbb{R}^n with covariance matrices $P_0, P_1 \in \mathbb{S}_{++}^n$, respectively. Define $p_t^{\text{info}}(\mathbf{x}), \mathbf{v}_t^{\text{info}}(\mathbf{x})$ as the minimizer of*

$$\inf_{p_t, \mathbf{v}_t} \left\{ 4 \int_0^1 \mathcal{E}_{p_t} \left(\|\mathbf{v}_t(\mathbf{x})\|_{P_t^{-1}}^2 \right) dt \mid \dot{p}_t + \nabla_{\mathbf{x}} \cdot (p_t \mathbf{v}_t) = 0 \right\}. \quad (27)$$

Then $p_t^{\text{info}}(\mathbf{x})$ is zero-mean Gaussian whose covariance matrix is equal to P_t^{info} from (1) and $\mathbf{v}_t^{\text{info}}(\mathbf{x}) = A^{\text{info}} \mathbf{x}$ almost surely with A^{info} given by (22). Moreover, the optimal value is equal to $d_{\text{info}}(P_0, P_1)^2$.

Proof. First, we define

$$\begin{bmatrix} V_t & C_t \\ C_t' & P_t \end{bmatrix} := \mathcal{E}_{p_t} \left(\begin{bmatrix} \mathbf{v}_t(\mathbf{x}) \\ \mathbf{x} \end{bmatrix} \begin{bmatrix} \mathbf{v}_t(\mathbf{x})' & \mathbf{x}' \end{bmatrix} \right). \quad (28)$$

Then applying integral by parts to obtain that

$$\begin{aligned} \dot{P}_t &= \int_{\mathbb{R}^n} \mathbf{x} \mathbf{x}' \dot{p}_t(\mathbf{x}) d\mathbf{x} \\ &= \int_{\mathbb{R}^n} -\mathbf{x} \mathbf{x}' \nabla \cdot (p_t(\mathbf{x}) \mathbf{v}_t(\mathbf{x})) d\mathbf{x} = C_t + C_t'. \end{aligned} \quad (29)$$

Therefore, the following optimization problem

$$\min_{C_t, V_t, P_t} \left\{ 4 \int_0^1 \text{tr}(P_t^{-1} V_t) dt \mid \begin{bmatrix} V_t & C_t \\ C_t' & P_t \end{bmatrix} \in \mathbb{S}_+^{2n \times 2n}, \right. \\ \left. \dot{P}_t = C_t + C_t' \right\} \quad (30)$$

provides a lower bound of (27) because the higher-order moments of the probability density functions are not considered. On the other hand, (25) provides an upper bound of (27) because the velocity field is constrained to satisfy the linear system. Then, we show that the two bounds coincide.

Note that $V_t - C_t P_t^{-1} C_t' \in \mathbb{S}_+^{n \times n}$. Thus the optimal V_t of (30) should satisfy that $V_t = C_t P_t^{-1} C_t'$.

Therefore, (30) is equal to

$$\min_{C_t, P_t \in \mathbb{S}_+^{n \times n}} \left\{ 4 \int_0^1 \text{tr}(P_t^{-1} C_t P_t^{-1} C_t') dt \mid \dot{P}_t = C_t + C_t' \right\}. \quad (31)$$

Note that the constrain $P_t \in \mathbb{S}_+^{n \times n}$ is automatically satisfied due to the inverse barrier objective function. Therefore, we drop the constraint that $P_t \in \mathbb{S}_+^{n \times n}$ in the following analysis.

Next, we consider the optimization problem (31) as an optimal control problem with C_t being matrix-valued control. Then we derive the optimal solution using Pontryagin's minimum principle. A necessary condition for the optimal solution is that it much annihilate the variation of the Hamiltonian

$$h_1(C_t, P_t, \Pi_t) := 4\text{tr}(P_t^{-1} C_t P_t^{-1} C_t') + \text{tr}(\Pi_t(C_t + C_t'))$$

with respect to the control C_t . Here, Π_t is a symmetric matrix representing the Lagrange multiplier, i.e. the co-state. By setting the partial derivative of $h_1(\cdot)$ with respect to C_t to zero, we obtain that

$$C_t = -\frac{1}{4} P_t \Pi_t P_t, \quad (32)$$

which provides a necessary condition that the optimal C_t is symmetric. Therefore $C_t = \frac{1}{2} \dot{P}_t$ and the objective function in (30) becomes $\text{tr}(P_t^{-1} \dot{P}_t P_t^{-1} \dot{P}_t) = \mathfrak{g}_{P, \text{Rao}}(\dot{P}_t)$. Thus, the theorem directly follows from (18). For completeness, we finish the proof based on the Hamiltonian $h_1(\cdot)$ in below.

The optimal $\dot{\Pi}_t$ must annihilate the partial derivative of $h_1(\cdot)$ with respect to P_t . This gives rise to

$$\dot{\Pi}_t = 8P_t^{-1} C_t P_t^{-1} C_t' P_t^{-1}. \quad (33)$$

Then, substituting (32) into (29) and (33) to obtain that

$$\begin{aligned} \dot{P}_t &= -\frac{1}{2} P_t \Pi_t P_t, \\ \dot{\Pi}_t &= \frac{1}{2} \Pi_t P_t \Pi_t. \end{aligned} \quad (34)$$

Note that $\dot{P}_t \Pi_t + P_t \dot{\Pi}_t = 0$ for all t . Hence $P_t \Pi_t$ is constant. We set

$$-\frac{1}{4} P_t \Pi_t = A. \quad (35)$$

Thus (32) is equal to $C_t = AP_t = P_t A'$. Multiplying both sides by $P_t^{-\frac{1}{2}}$ gives that $P_t^{-\frac{1}{2}} C_t P_t^{-\frac{1}{2}} = P_t^{-\frac{1}{2}} A P_t^{\frac{1}{2}}$ which is symmetric for all t . Substituting (35) to (34) to give that

$$\dot{P}_t = AP_t + P_t A'.$$

Therefore,

$$P_t = e^{At} P_0 e^{A't}.$$

Multiplying $P_0^{-\frac{1}{2}}$ to both sides to give

$$P_0^{-\frac{1}{2}} P_t P_0^{-\frac{1}{2}} = P_0^{-\frac{1}{2}} e^{At} P_0 e^{A't} P_0^{-\frac{1}{2}} = e^{2P_0^{-\frac{1}{2}} A P_0^{\frac{1}{2}} t}.$$

By setting $t = 1$, we solve that

$$A = \frac{1}{2} P_0^{\frac{1}{2}} \log(P_0^{-\frac{1}{2}} P_1 P_0^{-\frac{1}{2}}) P_0^{-\frac{1}{2}},$$

which is equal to A^{info} . Furthermore, from (23), the corresponding P_t is equal to P_t^{info} . Then the optimal covariance matrix in (28) is singular and has rank n . Thus the optimal velocity field $\mathbf{v}_t(\mathbf{x})$ is equal to $A^{\text{info}} \mathbf{x}$ almost surely, implying that the corresponding $p_t(\mathbf{x})$ is Gaussian. Therefore, the theorem is proved. \square

Note that the system matrix A^{info} is constant. Thus both A^{info} and A_t^{omt} have fixed eigenspaces. Next, we introduce a different quadratic form of A_t which leads to system matrices with rotating eigenspace.

IV. ROTATION-LINEAR-SYSTEM BASED COVARIANCE PATHS

A. Weighted-least-squares cost functions

Note that if X is an asymmetric matrix, i.e. $X' = -X$, then e^{Xt} is a rotation matrix. Consequently, if the system matrix A is asymmetric, then the state covariance matrix has a rotating eigenspace. In this regard, we decompose

$$A = A_s + A_a,$$

where $A_s := \frac{1}{2}(A + A')$, $A_a := \frac{1}{2}(A - A')$ are the symmetric and asymmetric parts of A , respectively. Then, we define the following weighted-least-squares (WLS) function

$$f_\epsilon(A) := \|A_s\|_F^2 + \epsilon \|A_a\|_F^2, \quad (36)$$

where the scalar $\epsilon > 0$ weighs the relative significance of symmetric and asymmetric parts of A . If A satisfies $\dot{P} = AP + PA'$ for a given pair \dot{P} and P , then $f_\epsilon(A)$ is considered as a quadratic form of the non-commutative division of \dot{P} by P , similar to the Fisher-Rao metric. Actually, for scalar-valued covariances, $f_\epsilon(A)$ is equal to the Fisher-Rao metric.

Following (5), we consider the optimal solution to

$$\min_{P_t, A_t} \left\{ \int_0^1 f_\epsilon(A_t) dt \mid \dot{P}_t = A_t P_t + P_t A'_t, P_0, P_1 \text{ specified} \right\}, \quad (37)$$

for a given pair of endpoints $P_0, P_1 \in \mathbb{S}_{++}^n$ and a scalar $\epsilon > 0$.

B. Optimal covariance paths

To introduce the solution to (37), we define

$$T_{\epsilon,t}(A) := e^{(1+\epsilon)A_a t} e^{(A_s + \epsilon A'_a)t}. \quad (38)$$

The next lemma shows that $T_{\epsilon,t}(\cdot)$ is equal to the state transition matrix of a linear time-varying system.

Lemma 2. *Given $A \in \mathbb{R}^{n \times n}$ and a scalar ϵ . Define*

$$A_{\epsilon,t} := e^{(1+\epsilon)A_a t} A e^{(1+\epsilon)A'_a t}.$$

Then

$$\dot{T}_{\epsilon,t}(A) = A_{\epsilon,t} T_{\epsilon,t}(A). \quad (39)$$

Proof.

$$\begin{aligned} \dot{T}_{\epsilon,t}(A) &= e^{(1+\epsilon)A_a t} ((1+\epsilon)A_a) e^{(A_s + \epsilon A'_a)t} + e^{(1+\epsilon)A_a t} (A_s + \epsilon A'_a) e^{(A_s + \epsilon A'_a)t} \\ &= e^{(1+\epsilon)A_a t} A e^{(A_s + \epsilon A'_a)t} = A_{\epsilon,t} T_{\epsilon,t}(A). \end{aligned}$$

□

The following corollary is a direct result of Lemma 2.

Corollary 1. *Given $P_0 \in \mathbb{S}_{++}^n$, $A \in \mathbb{R}^{n \times n}$ and a scalar ϵ . Define*

$$P_{\epsilon,t} := T_{\epsilon,t}(A)P_0T_{\epsilon,t}(A)'.$$

Then the following equation holds

$$\dot{P}_{\epsilon,t} = A_{\epsilon,t}P_{\epsilon,t} + P_{\epsilon,t}A_{\epsilon,t}. \quad (40)$$

Next, we are ready to present the solution to (37).

Proposition 4. *Given $P_0, P_1 \in \mathbb{S}_{++}^n$ and a scalar $\epsilon > 0$. If there exists a $\Pi_0 \in \mathbb{S}^n$ such that*

$$P_{\epsilon,t}^{\text{wls}} = T_{\epsilon,t}(A_0)P_0T_{\epsilon,t}(A_0)', \quad (41)$$

satisfies that $P_{\epsilon,1}^{\text{wls}} = P_1$ with

$$A_0 = -\frac{1}{2}(P_0\Pi_0 + \Pi_0P_0) - \frac{1}{2\epsilon}(\Pi_0P_0 - P_0\Pi_0), \quad (42)$$

and $T_{\epsilon,t}(\cdot)$ given by (38), then $P_{\epsilon,t}^{\text{wls}}$ is a minimizer of (37). The corresponding optimal A_t is equal to

$$A_{\epsilon,t}^{\text{wls}} = e^{(1+\epsilon)A_0t}A_0e^{(1+\epsilon)A_0't}. \quad (43)$$

Proof. Consider (37) as an optimal control problem with A_t being matrix-valued control. Then, the Hamiltonian is as follows

$$\begin{aligned} h_2(A_t, P_t, \Pi_t) &= \frac{1}{4}\|A_t + A_t'\|_{\mathbb{F}}^2 + \frac{\epsilon}{4}\|A_t - A_t'\|_{\mathbb{F}}^2 + \text{tr}(\Pi_t(A_tP_t + P_tA_t')), \\ &= \frac{1+\epsilon}{2}\text{tr}(A_tA_t') + \frac{1-\epsilon}{2}\text{tr}(A_tA_t) + \text{tr}(\Pi_t(A_tP_t + P_tA_t')). \end{aligned}$$

It is necessary that $\dot{\Pi}_t$ annihilates the partial derivative of $h_2(\cdot)$ with respect to P_t , which gives rise to

$$\dot{\Pi}_t = -\Pi_tA_t - A_t'\Pi_t. \quad (44)$$

Moreover, the partial derivative of $h_2(\cdot)$ with respect to the control A_t vanishes, which leads to

$$(A_t + A'_t) + \epsilon(A_t - A'_t) + 2\Pi_t P_t = 0. \quad (45)$$

Solving A_t from (45) to obtain that

$$A_t = -\frac{1}{2}(P_t \Pi_t + \Pi_t P_t) - \frac{1}{2\epsilon}(\Pi_t P_t - P_t \Pi_t). \quad (46)$$

Then, substituting (46) in (4) and (44), respectively, to obtain

$$\begin{aligned} \dot{P}_t &= (-1 + \frac{1}{\epsilon})P_t \Pi_t P_t - (\frac{1}{2} + \frac{1}{2\epsilon})(\Pi_t P_t^2 + P_t^2 \Pi_t), \\ \dot{\Pi}_t &= (1 - \frac{1}{\epsilon})\Pi_t P_t \Pi_t + (\frac{1}{2} + \frac{1}{2\epsilon})(\Pi_t^2 P_t + P_t \Pi_t^2). \end{aligned}$$

Next, it can be verified that $(\Pi_t \dot{P}_t) - (P_t \dot{\Pi}_t) = 0$. Thus, the asymmetric part of A_t , which is equal to

$$(A_t)_a = -\frac{1}{2\epsilon}(\Pi_t P_t - P_t \Pi_t),$$

is constant and denoted by A_a . Taking the derivative of its symmetric part

$$(A_t)_s = \frac{1}{2}(A_t + A'_t) = -\frac{1}{2}(P_t \Pi_t + \Pi_t P_t)$$

gives that

$$\begin{aligned} (\dot{A}_t)_s &= -\frac{1}{2}(\dot{P}_t \Pi_t) - \frac{1}{2}(\Pi_t \dot{P}_t) \\ &= \frac{1+\epsilon}{2\epsilon}(P_t \Pi_t^2 P_t - \Pi_t P_t^2 \Pi_t) \\ &= (1 + \epsilon)(A_a (A_t)_s + (A_t)_s A'_a). \end{aligned}$$

Since A_a is constant, the solution to the above equation is equal to

$$(A_t)_s = e^{(1+\epsilon)A_a t} A_s e^{(1+\epsilon)A'_a t}.$$

Therefore, the optimal A_t has the form

$$\begin{aligned} A_t &= e^{(1+\epsilon)A_a t} A_s e^{(1+\epsilon)A'_a t} + A_a, \\ &= e^{(1+\epsilon)A_a t} A e^{(1+\epsilon)A'_a t}, \end{aligned}$$

with $A = A_a + A_s$ being the initial value of A_t . Next, we define a new variable

$$\hat{P}_t := e^{(1+\epsilon)A'_a t} P_t e^{(1+\epsilon)A_a t}, \quad (47)$$

whose derivative is equal to

$$\begin{aligned} \dot{\hat{P}}_t &= e^{(1+\epsilon)A'_a t} (A_t P_t + P_t A'_t) e^{(1+\epsilon)A_a t} \\ &\quad + (1 + \epsilon) A'_a \hat{P}_t + \hat{P}_t (1 + \epsilon) A_a \\ &= (A_s + \epsilon A'_a) \hat{P}_t + \hat{P}_t (A_s + \epsilon A_a). \end{aligned}$$

Thus the solution to $\dot{\hat{P}}_t$ is equal to

$$\hat{P}_t = e^{(A_s + \epsilon A'_a)t} P_0 e^{(A_s + \epsilon A_a)t}.$$

Substituting this solution to (47) to obtain that the optimal P_t has the form

$$P_t = e^{(1+\epsilon)A_a t} e^{(A_s + \epsilon A'_a)t} P_0 e^{(A_s + \epsilon A_a)t} e^{(1+\epsilon)A'_a t}.$$

In a similar way, we define $\hat{\Pi}_t = e^{(1+\epsilon)A'_a t} \Pi_t e^{(1+\epsilon)A_a t}$. Then

$$\dot{\hat{\Pi}}_t = (-A_s + \epsilon A'_a) \hat{\Pi}_t + \hat{\Pi}_t (-A_s + \epsilon A_a),$$

whose solution is equal to

$$\hat{\Pi}_t = e^{(1+\epsilon)A_a t} e^{(-A_s + \epsilon A'_a)t} \Pi_0 e^{(-A_s + \epsilon A_a)t} e^{(1+\epsilon)A'_a t}. \quad (48)$$

If (42) holds, then $A_s + \epsilon A'_a = -P_0 \Pi_0$. It is straightforward to show that (46) holds for all $t > 0$ for the provided expressions for A_t, P_t, Π_t . In this case, $f_\epsilon(A_t) = \|A_s\|_F^2 + \epsilon \|A_a\|_F^2$ for all t . Therefore, if the A is equal to \hat{A} in (42), then the proposed trajectories $A_{\epsilon,t}^{\text{wls}}$ and $P_{\epsilon,t}^{\text{wls}}$ is local minimizer, which completes the proof. \square

Next, we provide an upper bound of the optimal value of (37) for all $\epsilon > 0$. For this purpose, we define

$$\hat{A} = \log(P_0^{-\frac{1}{2}} (P_0^{\frac{1}{2}} P_1 P_0^{\frac{1}{2}})^{\frac{1}{2}} P_0^{-\frac{1}{2}}),$$

which is symmetric. Moreover, $P_t = e^{\hat{A}t} P_0 e^{\hat{A}t}$ is a feasible solution to (37). Therefore, the following proposition holds

Proposition 5. Given $P_0, P_1 \in \mathbb{S}_{++}^n$ and a scalar $\epsilon > 0$. Then the optimal value of (37) is not larger than $\|\log(P_0^{-\frac{1}{2}}(P_0^{\frac{1}{2}}P_1P_0^{\frac{1}{2}})^{\frac{1}{2}}P_0^{-\frac{1}{2}})\|_F^2$.

C. On the existence and uniqueness of rotation-system based paths

We will analyze the existence of a covariance path of the form (41) that connects two given $P_0, P_1 \in \mathbb{S}_{++}^n$. To simplify notations, we denote $\alpha = (1 + \epsilon)/(2\epsilon)$. Furthermore, we remove the constraint that $\epsilon > 0$ and consider all $\epsilon \neq 0$. Based on the new parameter α , the closed-form equations (41), (42) and (43) have defined the following mapping

$$\begin{aligned} h_{\alpha, P_0}(\Pi) &: \mathbb{S}^n \rightarrow \mathbb{S}_{++}^n \\ &: \Pi \mapsto e^{\alpha(P_0\Pi - \Pi P_0)} e^{-P_0\Pi} P_0 e^{-\Pi P_0} e^{\alpha(\Pi P_0 - P_0\Pi)}. \end{aligned} \quad (49)$$

We will analyze the existence of Π that satisfies

$$h_{\alpha, P_0}(\Pi) = P_1, \quad (50)$$

for a given α . If there exists a $\Pi \in \mathbb{S}^n$ that solves (50) with $\alpha \neq \frac{1}{2}$, then there exists a covariance path of the form (41) with $\epsilon = 1/(2\alpha - 1)$.

In the special case when $\alpha = 0$, (50) becomes $e^{-P_0\Pi} P_0 e^{-\Pi P_0} = P_1$, which is equivalent to

$$\exp(-2P_0^{\frac{1}{2}}\Pi P_0^{\frac{1}{2}}) = P_0^{-\frac{1}{2}}P_1P_0^{-\frac{1}{2}}.$$

Clearly, it has a unique solution given by

$$\Pi_0 = -\frac{1}{2}P_0^{-\frac{1}{2}}\log(P_0^{-\frac{1}{2}}P_1P_0^{-\frac{1}{2}})P_0^{-\frac{1}{2}}. \quad (51)$$

It is interesting to note that the corresponding covariance path is equal to the Fisher-Rao-based geodesics P_t^{info} given by (1).

Because the mapping h_{α, P_0} is continuous in term of α and Π , it is expected that (50) also has a solution if α is sufficiently close to zero. Specifically, we assume that exists a solution Π to (50) for a specific α , e.g. $\alpha = 0$. Then, we can derive the following expression from (50)

$$\Pi = -\frac{1}{2}P_0^{-\frac{1}{2}}\log(P_0^{-\frac{1}{2}}e^{\alpha(\Pi P_0 - P_0\Pi)}P_1e^{\alpha(P_0\Pi - \Pi P_0)}P_0^{-\frac{1}{2}})P_0^{-\frac{1}{2}}. \quad (52)$$

Next, we will apply perturbation analysis to the above equation to understand the solutions associated with different values for α . Specifically, let δ_α and Δ_Π denote perturbations to α and

Π , respectively, so that $\alpha + \delta_\alpha$ and $\Pi + \Delta_\Pi$ still satisfy (52). Then, for small perturbations, the perturbation¹ of both sides of (52) gives rise to

$$\begin{aligned} \Delta_\Pi = & -\frac{1}{2}P_0^{-\frac{1}{2}}M_Q^{-1}\left(\alpha P_0^{-\frac{1}{2}}M_U(\Delta_\Pi P_0 - P_0\Delta_\Pi)P_1U'P_0^{-\frac{1}{2}}\right. \\ & + \alpha P_0^{-\frac{1}{2}}UP_1M_{U'}(P_0\Delta_\Pi - \Delta_\Pi P_0)P_0^{-\frac{1}{2}} \\ & + \delta_\alpha P_0^{-\frac{1}{2}}(\Pi P_0 - P_0\Pi)UP_1U'P_0^{-\frac{1}{2}} \\ & \left. + \delta_\alpha P_0^{-\frac{1}{2}}UP_1U'(P_0\Pi - \Pi P_0)P_0^{-\frac{1}{2}}\right)P_0^{-\frac{1}{2}} + o(|\delta_\alpha|) + o(\|\Delta_\Pi\|), \end{aligned} \quad (55)$$

where $o(|\delta_\alpha|) + o(\|\Delta_\Pi\|)$ denotes higher order terms of the perturbations,

$$\begin{aligned} U &= e^{\alpha(\Pi P_0 - P_0\Pi)}, \\ Q &= P_0^{-\frac{1}{2}}UP_1U'P_0^{-\frac{1}{2}}, \end{aligned}$$

and $M_X^{-1}(\cdot)$ and $M_X(\cdot)$ are defined in (53) and (54), respectively. Next, we combine all the terms containing Δ_Π on the right hand side of (55) to define the following linear mapping $\hat{h}_{\alpha, P_0, \Pi} : \mathbb{S}^n \rightarrow \mathbb{S}^n$,

$$\begin{aligned} \hat{h}_{\alpha, P_0, \Pi} : \Delta_\Pi \mapsto & -\frac{1}{2}P_0^{-\frac{1}{2}}M_Q^{-1}\left(P_0^{-\frac{1}{2}}M_U(\Delta_\Pi P_0 - P_0\Delta_\Pi)P_1U'P_0^{-\frac{1}{2}}\right. \\ & \left. + P_0^{-\frac{1}{2}}UP_1M_{U'}(P_0\Delta_\Pi - \Delta_\Pi P_0)P_0^{-\frac{1}{2}}\right)P_0^{-\frac{1}{2}}. \end{aligned} \quad (56)$$

Then the terms that containing the δ_α is equal to $\delta_\alpha \hat{h}_{\alpha, P_0, \Pi}(\Pi)$, Thus, (55) is equivalent to

$$(I - \alpha \hat{h}_{\alpha, P_0, \Pi})(\Delta_\Pi) = \delta_\alpha \hat{h}_{\alpha, P_0, \Pi}(\Pi) + o(|\delta_\alpha|) + o(\|\Delta_\Pi\|), \quad (57)$$

¹ For $A, \Delta \in \mathbb{R}^{n \times n}$,

$$e^{A+\Delta} = e^A + M_{e^A}(\Delta) + o(\|\Delta\|),$$

where $M_X(\Delta)$ denotes the non-commutative multiplication of Δ by X which is defined as

$$M_X(\Delta) = \int_0^1 X^{1-\tau} \Delta X^\tau d\tau. \quad (53)$$

For positive definite matrices $A, A + \Delta \in \mathbb{S}_{++}^n$,

$$\log(A + \Delta) = \log(A) + M_A^{-1}(\Delta) + o(\|\Delta\|),$$

where $M_X^{-1}(\Delta)$ denotes the non-commutative division of Δ by X which is defined as

$$M_X^{-1}(\Delta) = \int_0^\infty (X + \tau I)^{-1} \Delta (X + \tau I)^{-1} d\tau. \quad (54)$$

where I denotes the identity mapping.

Let $\alpha_\tau = \alpha\tau$ denote a smooth trajectory on the interval $\tau \in [0, 1]$ for a given α . If the linear mapping $I - \alpha\hat{h}_{\alpha_\tau, P_0, \Pi_\tau}$ is invertible, then solution to the following differential equation

$$\frac{d}{d\tau}\Pi_\tau = (I - \alpha_\tau\hat{h}_{\alpha_\tau, P_0, \Pi_\tau})^{-1} \circ \alpha\hat{h}_{\alpha_\tau, P_0, \Pi_\tau}(\Pi_\tau), \quad (58)$$

at $\tau = 1$ with the initial value given by Π_0 in (51) is equal to the unique solution to (50).

The following theorem provides a sufficient condition on the existence and uniqueness of the solution. To introduce the results, we let $\lambda_{\min}(P)$ and $\lambda_{\max}(P)$ denote the smallest and the largest eigenvalues of a matrix $P \in \mathbb{S}^n$. Moreover, we define the following pseudo-norm of a matrix $P \in \mathbb{S}^n$:

$$\|P\|_a := \max_{\Delta \in \mathbb{S}^n, \Delta \neq 0} \frac{\|\Delta P - P\Delta\|}{\|\Delta\|}. \quad (59)$$

Note that if P is equal to the identify matrix scaled by any scalar then $\|P\|_a = 0$. If $\|P\|_a = 0$, we follow the conventions to define $\lambda/\|P\|_a = +\infty$ for any $\lambda > 0$. Then, we obtain the following theorem.

Theorem 2. *For a pair of positive definite matrices $P_0, P_1 \in \mathbb{S}_{++}^n$, if α is a scalar such that*

$$|\alpha| < \max \left\{ \frac{\lambda_{\min}(P_0)\lambda_{\min}(P_1)}{\|P_0\|_a\lambda_{\max}(P_1)}, \frac{\lambda_{\min}(P_0)\lambda_{\min}(P_1)}{\|P_1\|_a\lambda_{\max}(P_0)} \right\}, \quad (60)$$

then there exists a unique $\Pi \in \mathbb{S}^n$ that satisfies

$$e^{\alpha(P_0\Pi - \Pi P_0)} e^{-P_0\Pi} P_0 e^{-\Pi P_0} e^{\alpha(\Pi P_0 - P_0\Pi)} = P_1.$$

Proof. Following (58), we will prove that $I - \alpha_\tau\hat{h}_{\alpha_\tau, P_0, \Pi_\tau}$ is invertible if (60) holds. It is sufficient to prove that the singular values of the symmetric mapping $\hat{h}_{\alpha_\tau, P_0, \Pi_\tau}$ are all smaller than 1. For this purpose, we will compute the norm of $h_{\alpha_\tau, P_0, \Pi_\tau}(\Delta_\Pi)$ defined by (56). The norm of the first

two terms containing Δ_Π is equal to

$$\begin{aligned}
& \frac{1}{2} \left\| P_0^{-\frac{1}{2}} M_Q^{-1} \left(P_0^{-\frac{1}{2}} M_U (\Delta_\Pi P_0 - P_0 \Delta_\Pi) P_1 U' P_0^{-\frac{1}{2}} \right) P_0^{-\frac{1}{2}} \right\| \\
&= \frac{1}{2} \left\| \int_0^\infty \int_0^1 P_0^{-\frac{1}{2}} (Q + t_1 I)^{-1} P_0^{-\frac{1}{2}} U^{1-t_2} (\Delta_\Pi P_0 - P_0 \Delta_\Pi) U^{t_2} P_1 U' P_0^{-\frac{1}{2}} (Q + t_1 I)^{-1} P_0^{-\frac{1}{2}} dt_1 dt_2 \right\| \\
&\leq \frac{1}{2} \int_0^\infty \left\| (P_0^{\frac{1}{2}} Q P_0^{\frac{1}{2}} + t_1 P_0)^{-1} \right\|^2 dt_1 \lambda_{\max}(P_1) \|P_0\|_a \|\Delta_\Pi\| \\
&\leq \frac{1}{2} \int_0^\infty (\lambda_{\min}(P_1) + t_1 \lambda_{\min}(P_0))^{-2} dt_1 \lambda_{\max}(P_1) \|P_0\|_a \|\Delta_\Pi\| \\
&\leq \frac{1}{2} \frac{\|P_0\|_a \lambda_{\max}(P_1)}{\lambda_{\min}(P_0) \lambda_{\min}(P_1)} \|\Delta_\Pi\|.
\end{aligned}$$

The same upper bound also holds for the other two terms containing Δ . Combining the bounds for all the four terms lead to

$$\|\alpha_\tau \hat{h}_{\alpha_\tau, P_0, \Pi_\tau}\| \leq \alpha \frac{\|P_0\|_a \lambda_{\max}(P_1)}{\lambda_{\min}(P_0) \lambda_{\min}(P_1)}.$$

Therefore, if

$$|\alpha| < \frac{\lambda_{\min}(P_0) \lambda_{\min}(P_1)}{\|P_0\|_a \lambda_{\max}(P_1)}, \quad (61)$$

then $I - \alpha_\tau \hat{h}_{\alpha_\tau, P_0, \Pi_\tau}$ is invertible for all $\tau \in [0, 1]$. Thus, we have proved the first term on the r.h.s. of (60).

The second term can be obtained in a similar way by considering a time-reversal path from P_1 to P_0 . Specifically, if

$$|\alpha| < \frac{\lambda_{\min}(P_0) \lambda_{\min}(P_1)}{\|P_1\|_a \lambda_{\max}(P_0)}, \quad (62)$$

then (61) implies that there exist a unique $\Pi_1 \in \mathbb{S}^n$ such that the following time-reversal path

$$P_{\epsilon, (1-t)} = T_{\epsilon, t}(A_1) P_1 T_{\epsilon, t}(A_1)', \quad (63)$$

satisfies $P_{\epsilon, 0} = P_0$, where

$$A_1 = -\frac{1}{2}(P_1 \Pi_1 + \Pi_1 P_1) - \frac{1}{2}(\Pi_1 P_1 - P_1 \Pi_1). \quad (64)$$

Next, we follow (48) to define

$$\Pi_{\epsilon,(1-t)} = e^{(1+\epsilon)(A_1)_a t} e^{-(A_1)_s + \epsilon(A_1)'_a} t \Pi_1 e^{-(A_1)_s + \epsilon(A_1)_a} t e^{(1+\epsilon)(A_1)_a t}, \quad (65)$$

where $(A_1)_s$ and $(A_1)_a$ denote the symmetric and asymmetric part of A_1 , respectively. Let $\Pi_0 = -\Pi_{\epsilon,(1-t)}$. Then Π_0 satisfies the conditions in Proposition 4. Specifically, the path from (63) satisfies the time-forward equation $P_{\epsilon,t} = T_{\epsilon,t}(A_0)P_0T_{\epsilon,t}(A_0)'$ with A_0 given by (42). Therefore, the proof is complete. \square

D. On the computation of local solutions

If $|\alpha|$ is large so that $I - \alpha_\tau \hat{h}_{\alpha_\tau, P_0, \Pi_\tau}$ from (58) is not invertible for some $\tau \in [0, 1]$, then there may exist multiple solutions to (50). In below, we propose an approach to compute local solutions (50) based on an approximate initial value.

Specifically, we consider $\hat{\Pi}_0$ as an initial guess for the solution to (50). We assume that the true endpoint P_1 is close to $\hat{P}_1 = h_{\alpha, P_0}(\hat{\Pi}_0)$. By applying perturbation analysis, we obtain that if the pair $\hat{\Pi}_0 + \Delta_\Pi$ and $\hat{P}_1 + \Delta_P$ satisfy (50) then the perturbations should satisfy

$$\Delta_\Pi - \alpha \hat{h}_{\alpha, P_0, \hat{\Pi}}(\Delta_\Pi) + o(\|\Delta_\Pi\|) = -\frac{1}{2} P_0^{-\frac{1}{2}} M_Q^{-1} (P_0^{-\frac{1}{2}} U \Delta_P U' P_0^{-\frac{1}{2}}) P_0^{-\frac{1}{2}} + o(\|\Delta_P\|).$$

Next, we define a path $P_\tau = (1 - \tau)\hat{P}_1 + \tau P_1$ for $\tau \in [0, 1]$. Then, P_τ remains in \mathbb{S}_{++}^n and $\dot{P}_\tau = P_1 - \hat{P}_1$. If $I - \alpha \hat{h}_{\alpha, P_0, \hat{\Pi}}$ is invertible, then the solution to the following differential equation

$$\frac{d}{d\tau} \hat{\Pi}_\tau = (I - \alpha \hat{h}_{\alpha, P_0, \hat{\Pi}})^{-1} \left(-\frac{1}{2} P_0^{-\frac{1}{2}} M_Q^{-1} (P_0^{-\frac{1}{2}} U (P_1 - \hat{P}_1) U' P_0^{-\frac{1}{2}}) P_0^{-\frac{1}{2}} \right),$$

at $\tau = 1$ with the initial value given by $\hat{\Pi}_0$ provides a solution to (50). The solution may depend on the choice of the initial value $\hat{\Pi}_0$ as illustrated by the following example.

V. EXAMPLES

A. Interpolating covariance matrices

In this example, we highlight the difference between $P_{\epsilon,t}^{\text{wls}}$ and the other two types of trajectories, i.e. P_t^{omt} , P_t^{info} , using the following two matrices as the endpoints

$$P_0 = \begin{bmatrix} 1 & 0 \\ 0 & 2 \end{bmatrix}, P_1 = \begin{bmatrix} 2 & 0 \\ 0 & 1 \end{bmatrix}. \quad (66)$$

Applying Eqs. (1) and (2) we obtain that

$$P_t^{\text{omt}} = \begin{bmatrix} (1 + (\sqrt{2} - 1)t)^2 & 0 \\ 0 & (\sqrt{2} + (1 - \sqrt{2})t)^2 \end{bmatrix},$$

$$P_t^{\text{info}} = \begin{bmatrix} 2^t & 0 \\ 0 & 2^{1-t} \end{bmatrix},$$

which are all diagonal. On the other hand, if $\epsilon = 0$ in (42), there are infinitely many asymmetric matrices A_0^{wls} of the following form

$$A_0^{\text{wls}} = \begin{bmatrix} 0 & \pm \frac{(2k+1)\pi}{2} \\ \mp \frac{(2k+1)\pi}{2} & 0 \end{bmatrix},$$

that makes the objective function equal to zero. The corresponding covariance paths are equal to

$$P_{0,t}^{\text{wls}} = \begin{bmatrix} 1 + \sin^2\left(\frac{(2k+1)\pi t}{2}\right) & \pm \cos\left(\frac{(2k+1)\pi t}{2}\right) \sin\left(\frac{(2k+1)\pi t}{2}\right) \\ \pm \cos\left(\frac{(2k+1)\pi t}{2}\right) \sin\left(\frac{(2k+1)\pi t}{2}\right) & 1 + \cos^2\left(\frac{(2k+1)\pi t}{2}\right) \end{bmatrix},$$

which are not diagonal.

To understand the covariance paths corresponding to nonzero ϵ , we gradually increase ϵ from 0.001 to 0.2 and numerically compute the solution to (50) by using the *fmincon* function in MATLAB[®] to search for a symmetric matrix Π that minimizes the least-square error $\|h_{\frac{1+\epsilon}{2\epsilon}, P_0}(\Pi) - P_1\|_F$. In this procedure, we apply the minimizer corresponding to a smaller ϵ as the initial value of the next step with a larger ϵ . In the first step when $\epsilon = 0.001$, we choose two initial values for $\hat{\Pi}$ as

$$\hat{\Pi}_{\pm} = \pm \begin{bmatrix} 0 & \pm\pi \\ \pm\pi & 0 \end{bmatrix} \times 10^{-3},$$

respectively, so that the initial system matrices from (42) are approximately asymmetric. As ϵ increases, we obtain two branches of numerical minimizers whose residuals are around 10^{-9} .

Figure 1 illustrates the trajectories of the entries of $P_{\epsilon,t}^{\text{wls}}$ corresponding to three positive values of ϵ . The dashed and solid red lines illustrate the off-diagonal entry of the two branches of minimizers. As ϵ increases, the magnitude of the off-diagonal entry reduces. Fig. 2 illustrates the off-diagonal entry $A_a(1, 2)$ of the two branches of local minimizers at different ϵ . The two branches collapse into a unique one when ϵ passes a threshold value around 0.13.

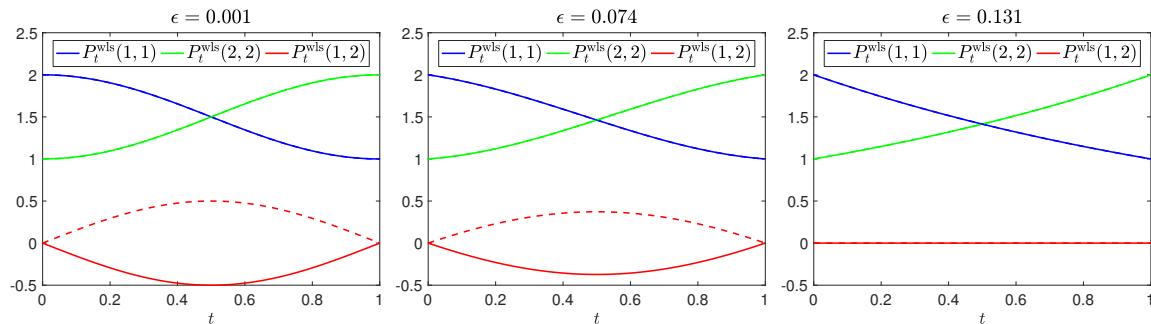


Fig. 1: An illustration of covariance paths $P_{\epsilon,t}^{wls}$ connecting P_0 and P_1 in (66) at three different values for ϵ .

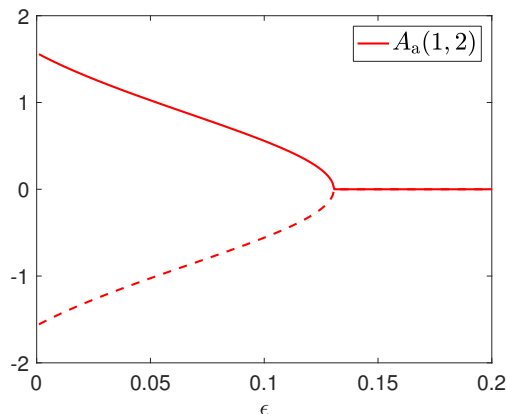


Fig. 2: An illustration of the off-diagonal entry $A_a(1,2)$ of two branches of local minimizers at different ϵ .

B. Regularization of sample covariances

We investigate an application to use the proposed covariance paths to fit noisy sample covariance matrices from a rsfMRI dataset. Below we provide detailed descriptions about the data, the method and experimental results.

1) *Data*: The sample covariances matrices are computed using a rsfMRI data set from the Human Connectome Project [31]. This dataset consists of 1200 rsfMRI image volumes measured in a 15-minute time window. The provided data has already been processed by the ICA-FIX method [32]. It is further processed using global signal regression (GSR) as suggested in [33]. Then we apply the label map from [35] to separate brain cortical surface into 7 non-overlapping regions. The data sequences from each region are averaged into a one-dimensional time series, providing a 7-dimensional time series sampled at 1200 time points. The same dataset and preprocessing method have been used in our early work [34]. Next, we normalize each dimension of the time series by its standard deviation. The normalized time series is denoted by

$\{\mathbf{x}_t, t = 1, \dots, 1200\}$. Moreover, we split the entire sequence into 10 equal-length segments and compute the corresponding sample covariance matrices as

$$\tilde{P}_k = \frac{1}{120} \sum_{i=1}^{120} \mathbf{x}_{120 \times k + i} \mathbf{x}'_{120 \times k + i}, \text{ for } k = 0, \dots, 9.$$

Then the time-scale is changed so that \tilde{P}_{t_k} is equal to \tilde{P}_k with $t_0 = 0$ and $t_9 = 1$. The color arrays in the first row of Fig. 3 illustrate several representative \tilde{P}_{t_k} at $t = 0, \frac{1}{3}, \frac{2}{3}, 1$, respectively. These figures show that \tilde{P}_{t_k} has significant fluctuations which is consistent to the observations from [11], [12]. The main goal of this proof-of-concept experiment is to use the proposed covariance paths to fit these sample covariances and compare their differences. The neuroscience aspects of this experiment will not be discussed in this paper.

2) *Method*: We solve optimization problems of the following form

$$\min_{P_t \in \mathcal{P}} \sum_{k=0}^K \|P_{t_k} - \tilde{P}_{t_k}\|_{\mathbb{F}}^2, \quad (67)$$

to obtain smooth paths that fit the measurements, where $K = 9$ and \mathcal{P} represents a suitable set of smooth paths. Based on results from the previous sections, we propose three sets of parametric models for the smooth paths which are described in below.

Based on Proposition 1, we define

$$\mathcal{P}_{\text{omt}} := \left\{ P_t \mid P_t = (I - tQ)P_0(I - tQ'), \right. \\ \left. P_0 \in \mathbb{S}_{++}^n, Q \in \mathbb{R}^{n \times n} \right\}.$$

Note that Q could be a non-symmetric matrix so that \mathcal{P}_{omt} contains the OMT-based geodesics in the form of (2). We use this more general family of covariance paths in order to obtain better fitting results. It is also clear from Proposition 1 that a $P_t \mathcal{P}_{\text{omt}}$ is the state covariance of a linear time varying system with $A_t = -Q(I - Qt)^{-1}$. We apply the *fminsdp* function² in MATLAB[®] to obtain an optimal solution. The initial values for P_0 and M are set to \tilde{P}_0 and the zero matrix, respectively. The same initial values and optimization algorithm are used to solve the subsequent optimization problems. The corresponding optimal value is denoted by \hat{P}_t^{omt} .

²This package is available from <https://www.mathworks.com/matlabcentral/fileexchange/43643-fminsdp>.

The second set of smooth paths is defined based on Proposition 2 which is given by

$$\mathcal{P}_{\text{info}} := \left\{ P_t \mid P_t = e^{At} P_0 e^{A't}, P_0 \in \mathbb{S}_{++}^n, A \in \mathbb{R}^{n \times n} \right\}.$$

$\mathcal{P}_{\text{info}}$ includes all geodesic paths in the form of P_t^{info} . The optimal path in this set is denoted by \hat{P}_t^{info} . Clearly, a trajectory in $P_t \in \mathcal{P}_{\text{info}}$ is equal to the state covariance of a linear time-invariant system.

Based on Proposition 4, we define

$$\mathcal{P}_{\epsilon, \text{wls}} := \left\{ P_t \mid P_t = T_{\epsilon, t}(A) P_0 T_{\epsilon, t}(A)', \right. \\ \left. P_0 \in \mathbb{S}_{++}^n, A \in \mathbb{R}^{n \times n} \right\},$$

for a given $\epsilon > 0$. The corresponding optimal paths are denoted by $\hat{P}_{\epsilon, t}^{\text{wls}}$. This set includes all the trajectories that are solutions of (37). A trajectory in $\mathcal{P}_{\epsilon, \text{wls}}$ is equal to the state covariance of a linear time-varying system with the system matrices expressed in the form $e^{(1+\epsilon)Aa t} A e^{(1+\epsilon)A'a t}$. The system matrices corresponding to $\hat{P}_{\epsilon, t}^{\text{wls}}$ is denoted by $\hat{A}_{\epsilon, t}^{\text{wls}}$. The parameter ϵ is then searched over a discrete set in $[0, 100]$ to minimize fitting errors. Based on the fitting results, we set the value of ϵ at 20.

3) *Results:* Figure 4 illustrates the fitting results of 6 representative entries of \tilde{P}_{t_k} . The black stars represent the noisy measurements. The blue, green, and red plots represent the estimated paths \hat{P}_t^{omt} , \hat{P}_t^{info} and $\hat{P}_{\epsilon, t}^{\text{wls}}$, respectively. \hat{P}_t^{omt} and \hat{P}_t^{info} are very similar with each other. Clearly, $\hat{P}_{\epsilon, t}^{\text{wls}}$ has more oscillations which better fits the fluctuations in the measurements. The normalized square errors $\left(\sum_{k=0}^K \|\hat{P}_{t_k} - \tilde{P}_{t_k}\|_{\text{F}}^2 \right) / \left(\sum_k \|\tilde{P}_{t_k}\|_{\text{F}}^2 \right)$ corresponding to \hat{P}_t^{omt} , \hat{P}_t^{info} , $\hat{P}_{\epsilon, t}^{\text{wls}}$ are equal to 0.1683, 0.1671, 0.1543, respectively. Thus, $\hat{P}_{\epsilon, t}^{\text{wls}}$ has the smallest fitting error. The overall relative large residual is partly due to the low-signal-to-noise ratio of fMRI data [36]. Therefore, the corresponding system matrices $\hat{A}_{\epsilon, t}^{\text{wls}}$ could better explain the dynamic interdependence between brain regions. The directed networks in the second row of Fig. 3 illustrates the matrices $\hat{A}_{\epsilon, t}^{\text{wls}}$ at $t = 0, \frac{1}{3}, \frac{2}{3}, 1$, respectively. The red and blue colors represent positive and negative values, respectively. The edge widths are weighted by the absolute value of the corresponding entries. To simplify visualization, edges with weight smaller than 0.15 are not displayed.

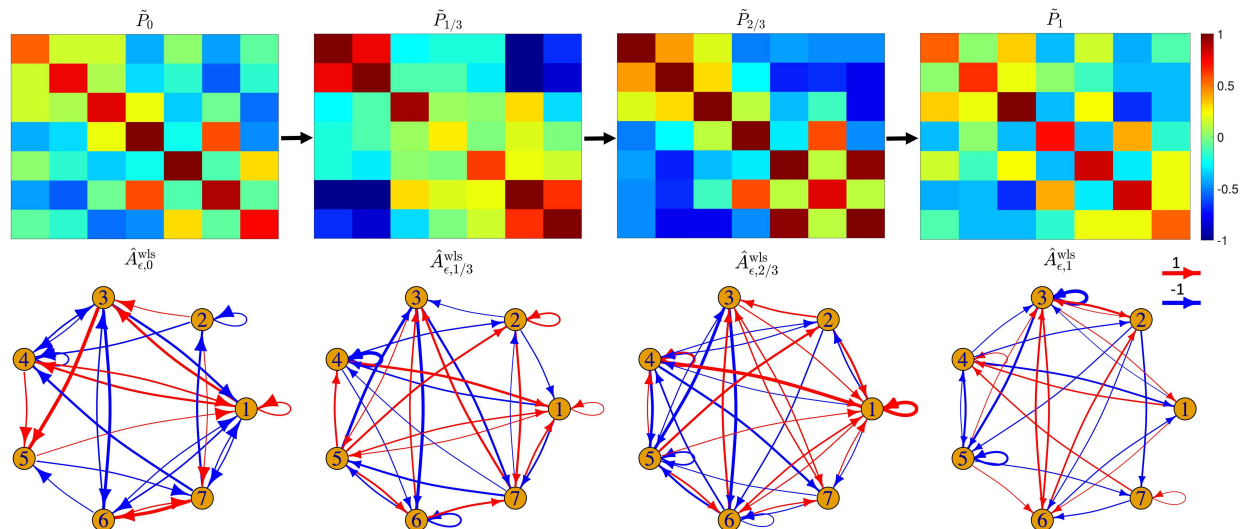


Fig. 3: The first row illustrates the sample covariance matrices between 7 brain regions computed from different segments of a rsfMRI data set from a human brain. The directed networks in the second row illustrate the estimated system matrices corresponding to the proposed weighted-least-squares trajectories.

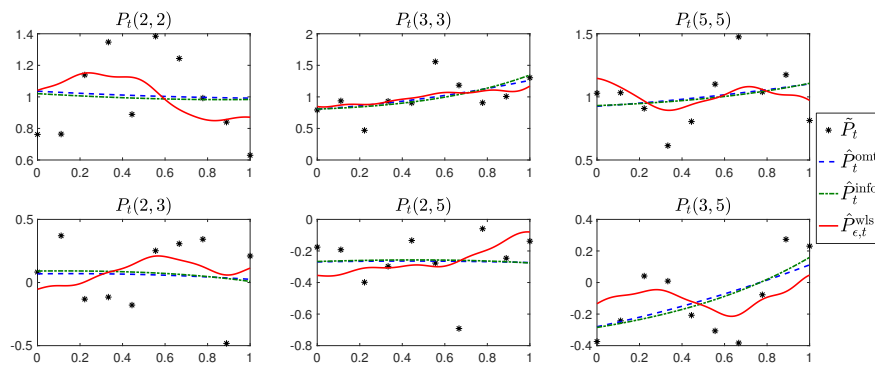


Fig. 4: The black stars in each image panel illustrate the noisy sample covariances matrices at different time points. The blue, green and red lines are the fitted curves using the proposed three sets of smooth paths.

VI. DISCUSSION

In this paper, we have investigated a framework to derive covariance paths on the Riemannian manifold of positive definite matrices by using quadratic forms of system matrices to regularize the path lengths. We have considered three types of quadratic forms and derived the corresponding covariance paths. The first and the second quadratic forms lead to the well-known geodesics derived from the Bures-Wasserstein metric from OMT and the Fisher-Rao metric from information geometry, respectively. In the process, we have derived a fluid-mechanics interpretation of the Fisher-Rao metric in Theorem 1, which provides an interesting weighted-mass-transport view

for the Fisher-Rao metric.

The third type of quadric form gives rise to a general family of covariance paths that are steered by system matrices with a rotating eigenspace. The rotation velocity is related to the choice of the parameter ϵ . In the special case when $\epsilon = -1$, i.e. $\alpha = 0$, then the eigenspace is not rotating and the trajectories reduce to the Fisher-Rao based geodesics. We also analyzed the existence and uniqueness of the paths with sufficiently small α .

We note that similar types of trajectories of positive definite matrices with rotating eigenspaces have been investigated in [37]–[39] from different angles. This work is developed along similar lines as [40], [41], which focus on the optimal steering of state covariances via linear systems using external input. But the approach for developing covariance paths used in this paper is different from early work.

In a proof-of-concept example, we apply three types of smooth paths of state covariance to fit noisy sample covariance matrices from a rsfMRI data set. A goal of this experiment is to understand directed interactions among brain regions via the estimated system matrices. As expected, the rotation-system-based covariance path has the best performance in terms of fitting fluctuations in the measurements. Therefore, the corresponding system matrices could provide a data-driven tool to understand the structured fluctuations of functional brain activities. In future work, we will apply this approach to analyze more complex brain networks using different path fitting algorithms. Moreover, we will also explore the proposed covariance paths to analyze data from other neuroimaging modalities such as EEG/MEG.

ACKNOWLEDGMENT

The author would like to thank Tryphon T. Georgiou and Yogesh Rathi for insightful discussions.

This work was supported in part under grants R21MH115280 (PI: Ning), R01MH097979 (PI: Rathi), R01MH11917 (PI: Rathi), R01MH074794 (PI: Westin).

REFERENCES

- [1] F. Porikli, O. Tuzel, and P. Meer, “Covariance tracking using model update based on lie algebra,” in *2006 IEEE Computer Society Conference on Computer Vision and Pattern Recognition (CVPR’06)*, vol. 1, June 2006, pp. 728–735.
- [2] Y. Wu, J. Cheng, J. Wang, H. Lu, J. Wang, H. Ling, E. Blasch, and L. Bai, “Real-time probabilistic covariance tracking with efficient model update,” *IEEE Transactions on Image Processing*, vol. 21, no. 5, pp. 2824–2837, May 2012.
- [3] J. F. Yang and M. Kaveh, “Adaptive eigensubspace algorithms for direction or frequency estimation and tracking,” *IEEE Transactions on Acoustics, Speech, and Signal Processing*, vol. 36, no. 2, pp. 241–251, Feb 1988.

- [4] X. Jiang, L. Ning, and T. T. Georgiou, “Distances and riemannian metrics for multivariate spectral densities,” *IEEE Transactions on Automatic Control*, vol. 57, no. 7, pp. 1723–1735, July 2012.
- [5] C. Lenglet, M. Rousson, R. Deriche, and O. Faugeras, “Statistics on the manifold of multivariate normal distributions: Theory and application to diffusion tensor MRI processing,” *Journal of Mathematical Imaging and Vision*, vol. 25, no. 3, pp. 423–444, Oct 2006. [Online]. Available: <https://doi.org/10.1007/s10851-006-6897-z>
- [6] I. L. Dryden, A. Koloydenko, and D. Zhou, “Non-euclidean statistics for covariance matrices, with applications to diffusion tensor imaging,” *The Annals of Applied Statistics*, vol. 3, no. 3, pp. 1102–1123, 2009. [Online]. Available: <http://www.jstor.org/stable/30242879>
- [7] X. Hao, R. T. Whitaker, and P. T. Fletcher, *Adaptive Riemannian Metrics for Improved Geodesic Tracking of White Matter*. Berlin, Heidelberg: Springer Berlin Heidelberg, 2011, pp. 13–24. [Online]. Available: https://doi.org/10.1007/978-3-642-22092-0_2
- [8] B. Biswal, F. Zerrin Yetkin, V. M. Haughton, and J. S. Hyde, “Functional connectivity in the motor cortex of resting human brain using echo-planar mri,” *Magnetic Resonance in Medicine*, vol. 34, no. 4, pp. 537–541, 1995. [Online]. Available: <http://dx.doi.org/10.1002/mrm.1910340409>
- [9] R. L. Buckner, F. M. Krienen, and B. T. T. Yeo, “Opportunities and limitations of intrinsic functional connectivity MRI,” *Nature Neuroscience*, vol. 16, pp. 832–837, 2013.
- [10] S. M. Smith, D. Vidaurre, C. F. Beckmann, and et al., “Functional connectomics from resting-state fMRI,” *Trends in Cognitive Sciences*, vol. 17, no. 12, pp. 666–682, 2013.
- [11] C. Chang and G. H. Glover, “Time-frequency dynamics of resting-state brain connectivity measured with fMRI,” *NeuroImage*, vol. 50, no. 1, pp. 81 – 98, 2010.
- [12] M. G. Preti, T. A. Bolton, and D. V. D. Ville, “The dynamic functional connectome: State-of-the-art and perspectives,” *NeuroImage*, vol. 160, pp. 41 – 54, 2017, functional Architecture of the Brain.
- [13] C. Rao, “Information and the accuracy attainable in the estimation of statistical parameters,” *Bull. Calcutta Math. Soc.*, vol. 37, pp. 81 – 91, 1945.
- [14] S.-I. Amari and H. Nagaoka, *Methods of information geometry*. Amer. Math. Soc., 2000.
- [15] N. Cencov, *Statistical decision rules and optimal inference*. Amer. Math. Soc., 1982.
- [16] R. Kass and P. Vos, *Geometrical foundations of asymptotic inference*. Wiley New York, 1997.
- [17] C. Villani, *Topics in Optimal Transportation*. Amer. Math. Soc., 2003.
- [18] S. Rachev and L. Rüschendorf, *Mass transportation problems. Vol. I and II. Probability and its Applications*. Springer, New York, 1998.
- [19] M. Knott and C. S. Smith, “On the optimal mapping of distributions,” *Journal of Optimization Theory and Applications*, vol. 43, no. 1, pp. 39–49, May 1984.
- [20] A. Takatsu, “On Wasserstein geometry of the space of Gaussian measures,” *ArXiv e-prints*, Jan. 2008.
- [21] A. Uhlmann, “The metric of bures and the geometric phase,” in *Quantum Groups and Related Topics: Proceedings of the First Max Born Symposium*, R. Gielerak, J. Lukierski, and Z. Popowicz, Eds., 1992, p. 267.
- [22] D. Petz, “Geometry of canonical correlation on the state space of a quantum system,” *Journal of Mathematical Physics*, vol. 35, pp. 780 – 795, 1994.
- [23] L. Ning, X. Jiang, and T. Georgiou, “On the geometry of covariance matrices,” *IEEE Signal Processing Letters*, vol. 20, no. 8, pp. 787–790, Aug 2013.
- [24] R. Bhatia, T. Jain, and Y. Lim, “On the Bures-Wasserstein distance between positive definite matrices,” *ArXiv e-prints*, Dec. 2017.

- [25] R. Jordan, D. Kinderlehrer, and F. Otto, “The variational formulation of the Fokker–Planck equation,” *SIAM Journal on Mathematical Analysis*, vol. 29, no. 1, pp. 1–17, 1998.
- [26] J.-D. Benamou and Y. Brenier, “A computational fluid mechanics solution to the monge-kantorovich mass transfer problem,” *Numerische Mathematik*, vol. 84, no. 3, pp. 375–393, Jan 2000.
- [27] S. Kullback and R. A. Leibler, “On information and sufficiency,” *The Annals of Mathematical Statistics*, vol. 22, no. 1, pp. 79–86, 1951.
- [28] T. Cover and J. Thomas, *Elements of Information Theory*. Wiley-Interscience, 2008.
- [29] R. Bhatia, *Positive definite matrices*. Princeton University Press, 2007.
- [30] T. T. Georgiou, “Relative entropy and the multivariable multidimensional moment problem,” *IEEE Transactions on Information Theory*, vol. 52, no. 3, pp. 1052–1066, 2006.
- [31] D. V. Essen, K. Ugurbil, E. Auerbach, and et al., “The human connectome project: A data acquisition perspective,” *NeuroImage*, vol. 62, no. 4, pp. 2222 – 2231, 2012, connectivity.
- [32] S. M. Smith, C. F. Beckmann, J. Andersson, and et al., “Resting-state fmri in the human connectome project,” *NeuroImage*, vol. 80, pp. 144 – 168, 2013, mapping the Connectome.
- [33] M. Fox, D. Zhang, A. Snyder, and M. Raichle, “The global signal and observed anticorrelated resting state brain networks,” *J. Neurophysiol.*, vol. 101, p. 3270?3283, 2009.
- [34] L. Ning and Y. Rathi, “A dynamic regression approach for frequency-domain partial coherence and causality analysis of functional brain networks,” *IEEE Transactions on Medical Imaging*, vol. PP, no. 99, pp. 1–1, 2017.
- [35] B. T. Yeo, F. M. Krienen, J. Sepulcre, M. R. Sabuncu, D. Lashkari, M. Hollinshead, J. L. Roffman, J. W. Smoller, L. Zöllei, J. R. Polimeni, B. Fischl, and R. Liu, H a.nd Buckner, “The organization of the human cerebral cortex estimated by intrinsic functional connectivity,” *J. Neurophysiol.*, vol. 106, pp. 1125–1165, 2011.
- [36] K. Murphy, J. Bodurka, and P. A. Bandettini, “How long to scan? the relationship between fmri temporal signal to noise ratio and necessary scan duration,” *NeuroImage*, vol. 34, no. 2, pp. 565 – 574, 2007.
- [37] L. Ning, T. T. Georgiou, and A. Tannenbaum, “On matrix-valued monge-kantorovich optimal mass transport,” *IEEE Transactions on Automatic Control*, vol. 60, no. 2, pp. 373–382, Feb 2015.
- [38] K. Yamamoto, Y. Chen, L. Ning, T. T. Georgiou, and A. Tannenbaum, “Regularization and interpolation of positive matrices,” *IEEE Transactions on Automatic Control*, vol. PP, no. 99, pp. 1–1, 2017.
- [39] Y. Chen, T. Georgiou, and A. Tannenbaum, “Matrix Optimal Mass Transport: A Quantum Mechanical Approach,” *ArXiv e-prints*, Oct. 2016.
- [40] Y. Chen, T. T. Georgiou, and M. Pavon, “Optimal steering of a linear stochastic system to a final probability distribution, Part I,” *IEEE Transactions on Automatic Control*, vol. 61, no. 5, pp. 1158–1169, May 2016.
- [41] —, “Optimal steering of a linear stochastic system to a final probability distribution, Part II,” *IEEE Transactions on Automatic Control*, vol. 61, no. 5, pp. 1170–1180, May 2016.
- [42] J. Geweke, “Measurement of linear dependence and feedback between multiple time series,” *J. Am Stat Assoc*, vol. 77, no. 378, pp. 304–313, 1982.